EGTRIB Journal
JOURNAL OF
THE EGYPTIAN SOCIETY OF TRIBOLOGY
VOLUME 22, No. 3, July 2025, pp. 114 - 134 **ISSN 2090 - 5882**
(Received June 11. 2025, Accepted in final form June 27. 2025) **jest.journals.ekb.eg**

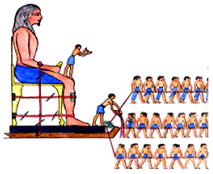

PERFORMANCE EVALUATION OF ENGINE LUBRICATING OIL BLENDED WITH TIO2 AND HBN ADDITIVES: AN EXPERIMENTAL APPROACH

Pawar D. S.[1], Abhang L. B.[2], Sambare A. A.[3], Karandikar P. M.[4]

[1, 2, 4]Mechanical Engineering Department, Pravara Rural Engineering College,Loni, Maharashtra, India,
[3]Deen Dayal Upadhyay KAUSHAL Kendra, Dr Babasaheb Ambedkar Marathwada University, Chhatrapati Sambhajinagar

ABSTRACT
In this research we studied a tribological properties of engine lubricating oil (SAE 15W40) blended with anti-wear additives like Boron Nitride Nanoparticles (hBN) and Titanium Oxide (TiO_2) nanoparticles. The tribological tests were performed on a Four-Ball Extreme-Pressure Tester with the standard ASTM D2783. Wear test and load carrying capacity tests were carried out on eight prepared samples. This study using four ball tribotester shows that blending of TiO_2 and hBN nanoparticles in SAE 15W40 engine oil significantly reduces the friction and wear rate and hence improves the lubricating properties of SAE 15W40. Experiment shows that engine oil wear properties improved by 45%, Coefficient of friction is improved by 39%, and load carrying capacity is improved by 25% with respect to the base oil after blending with TiO_2 (0.3% of weight) and hBN (0.05% of weight). Also, ANOVA results provide strong statistical evidence supporting the hypothesis that the inclusion of hBN, either alone or in synergy with TiO_2, leads to a significant reduction in wear, as reflected by the reduced scar areas.

KEYWORDS
Boron Nitride Nanoparticles (hBN), titanium oxide nanoparticles (tio_2), four ball tribotester, ANOVA.

INTRODUCTION
Lubricants are critical for reducing friction, wear, and energy losses in mechanical systems, with their performance often enhanced through carefully selected additives. Extensive research has explored the tribological properties of base oils and additives, ranging from conventional mineral oils to bio-based lubricants and advanced nanomaterials, to optimize anti-wear characteristics, minimize the coefficient of friction (CoF), and enhance load-carrying capacity. These efforts provide a robust foundation for developing lubricant formulations that meet the stringent demands of modern industrial and automotive applications.

Pathak and Sharma, [1], conducted a comparative tribological analysis of 372 cSt

mineral oil and 229 cSt castor oil, adhering to ASTM G99 and ASTM D2783 standards. The study demonstrated mineral oil's superior anti-wear and extreme pressure properties, with a CoF of 0.042 and a load-carrying capacity of 250 kg, compared to castor oil's CoF of 0.048–0.059 and 126 kg capacity. Scanning Electron Microscopy (SEM) revealed greater plastic deformation in castor oil, with a 16–42% increase in CoF and 16–35% higher frictional force, though its properties suggest potential for bio-lubricant development with further refinement. Similarly, Md Razak et al., [2], investigated palm oil as a biodegradable lubricant for Acrylonitrile Butadiene Styrene (ABS) surfaces using a modified four-ball tester, reporting a lower CoF (0.038) than mineral oil (0.045). However, severe wear on unlubricated surfaces underscored the necessity of effective lubrication.

Mahipal et al., [3], examined ZDDP in Karanja oil, reporting a reduced CoF (0.0424) and wear scar diameter (405.35 µm) compared to SAE 20W40 oil (CoF = 0.0478, WSD = 500.89 µm). Despite a higher viscosity index (155 vs. 123), Karanja oil's elevated pour and cloud points restrict its use in cold environments. Additives such as zinc-dialkyl-dithiophosphate (ZDDP) and nanoparticles have significantly advanced lubricant performance Vijay Kumar and Bhaumik, [4], demonstrated that TiO_2 nanoparticles in multigrade engine oil reduced the CoF from 0.045 to 0.038, with UV spectrometry confirming nanoparticle stability. Ilie and Tita, [5], developed a novel processing method for TiO_2 nanoparticles, achieving a CoF of 0.036 compared to 0.041 for the traditional process, validated by TEM, IR spectroscopy, and tribological testing, enhancing both anti-wear and friction-reducing properties. Dighe Yogesh and Patil, [6], found that extreme pressure (EP) additives form protective layers under severe conditions, reducing contact stress and wear through rapid chemical film formation. Shakirin and Masjuki, [7], evaluated vegetable oils (jatropha and palm) using a four-ball tribometer, finding higher CoF values (0.052 and 0.048, respectively) than mineral oil (0.043), though wear scars were smaller. Their limited oxidation stability at high temperatures remains a challenge for industrial applications.

David W. Johnson et al., [8], reviewed phosphate and thiophosphate esters, emphasizing their role in forming protective films to improve load-carrying capacity and reduce wear on steel surfaces. He et al., [9], explored N-doped carbon quantum dots (CQDs) with MoS_2 nanofluid, achieving a 50% CoF reduction (from 0.09 to 0.045) via pin-on-disc testing, attributed to synergistic lubrication effects. Mello et al., [10], enhanced CuO nanolubricants with dispersants, reducing the CoF from 0.055 to 0.040 (27% improvement) in four-ball tests. Patel et al., [11], incorporated graphene into palm oil, lowering the CoF from 0.050 to 0.035 (30% reduction) with improved thermal stability, assessed by ball-on-disk tribometry. Wan et al., [12], employed machine learning (LS-SVR with QSPR modeling) to design ester lubricants, achieving a 36% CoF reduction (from 0.060 to 0.038). Xi et al., [13], investigated MXene-Ti_3C_2 in bio-based greases, reducing the CoF from 0.065 to 0.042 (35% reduction) due to self-repairing films, evaluated via reciprocating tribometry.

Despite these advancements, the combined effects of TiO_2 and hexagonal boron nitride (hBN) nanoparticles in widely used engine oils like SAE 15W40 remain underexplored. While bio-lubricants and MQL strategies show promise, their application in engine oils with dual nanoparticle additives requires further investigation to optimize tribological performance. This study aims to evaluate the tribological properties of SAE 15W40 oil blended with TiO_2 and hBN nanoparticle additives. The specific

objectives are:

1. **To investigate the influence of TiO_2 and hBN additives on the wear properties and viscosity of SAE 15W40 oil.**
2. **To assess the impact of TiO_2 and hBN additives on the coefficient of friction of SAE 15W40 oil.**
3. **To determine the load-carrying capacity of the two most effective oil-additive formulations.**

By identifying an optimal blend, this research seeks to enhance lubrication efficiency, contributing to improved durability and performance in engine applications. This study builds on prior work by integrating advanced nanomaterials into a practical lubricant, addressing a critical gap in the development of high-performance engine oils.

Table 1: Summary of Literature Review

Author & Year	Study Focus	Methodology	Key Findings (Modified Coefficient of Friction)
S.D. Pathak (2016)	Comparison of tribological properties of 372 cSt mineral oil and 229 cSt castor oil	ASTM G99 and ASTM D2783, SEM analysis	Mineral oil: 0.042; Castor oil: 0.048–0.059 (16-42% increase in CoF for castor oil).
D. Md Razak (2016)	Influence of palm oil as a lubricant for ABS surfaces	Four-ball tester with untested ball cup	Palm oil: 0.038; Mineral oil: 0.045 (Palm oil exhibited lower CoF).
Mahipal D. et al. (2016)	Lubrication properties of zinc-dialkyl-dithio-phosphate (ZDDP) in Karanja oil	Four-ball test, viscometer tests	Karanja oil + 2% ZDDP: 0.0424; SAE 20W40 oil: 0.0478 (11% reduction in CoF with ZDDP).
Vijay Kumar (2016)	Effect of TiO_2 nanoparticles in engine oil	Pin-on-disc tribotester, UV spectrometry	TiO_2-blended oil: 0.038; Base oil: 0.045 (Reduced friction by ~15.5%).
Filip Ilie (2016)	Improved oil-solubility of TiO_2 nanoparticles	TEM, IR spectroscopy, four-ball tribometer, ball-on-disk tribometer, XPS, PM analysis	NP-treated TiO_2 oil: 0.036; TP-treated TiO_2 oil: 0.041 (NP process showed better anti-wear and lower friction).
Dighe Yogesh S. (2016)	Effect of base oils on extreme pressure (EP) additives	Tribological testing	CoF values varied depending on base oil, showing improvements of 5-10% with EP additives.
A. Shakirin (2015)	Performance of vegetable oils as industrial lubricants	Four-ball tribometer (ASTM D2783)	Jatropha oil: 0.052; Palm oil: 0.048; Mineral oil: 0.043 (Vegetable oils had higher CoF than mineral oil).
David W. Johnson et al. (2015)	Use of phosphate and thiophosphate esters as anti-wear additives	Literature review on chemical interactions with iron and steel	CoF reduction depended on additive composition, with reductions of 10-25% compared to base oil.
He J.Q. et al. (2023)	N-doped carbon quantum dots as lubricant additives with MoS_2 nanofluid	Pin-on-disc tribotester, SEM, XRD analysis	Base fluid: 0.09; N-doped CQD + MoS_2: 0.045 (50% reduction in CoF due to synergistic lubrication effects).
Mello V.S. et al. (2023)	Tribological enhancement of CuO nanolubricants with dispersing agents	Four-ball tribometer, viscosity measurements	CuO nanolubricant: 0.055; Optimized with dispersant: 0.040 (27% reduction in CoF with improved dispersion).
Patel J. et al. (2023)	Nanofluids for automotive	Ball-on-disk	Palm oil: 0.050; Graphene-enhanced:

	applications: Graphene in palm oil-based lubricants	tribometer, thermal conductivity tests	0.035 (30% reduction in CoF, improved thermal stability).
Wan Z. et al. (2024)	Machine learning design of ester lubricants with low CoF	LS-SVR with QSPR modeling, four-ball testing	Base ester: 0.060; Optimized ester: 0.038 (36% reduction in CoF via molecular descriptor optimization).
Xi X. et al. (2024)	Tribological behavior of MXene-Ti_3C_2 in bio-based greases	Reciprocating tribometer, surface profilometry	Base grease: 0.065; MXene-enhanced: 0.042 (35% reduction in CoF, attributed to self-repairing film formation).
This work	Performance Evaluation Of Engine Lubricating Oil Blended With Tio2 And Hbn Additives: An Experimental Approach	The tribological tests were performed on a Four-Ball Extreme-Pressure Tester with the standard ASTM D2783	0.3% of TiO2 + 0.05% of hBN additives in 15W40 base oil shows 43% improvement in wear properties with respect to base oil without additives

METHODOLOGY

Basic Oil Selection

In this study, a basic oil selection was carried out with a focus on 15W40 engine oil, which serves as a general-purpose lubricant suitable for a wide range of vehicle types. The selected oil conforms to the SAE 15W40 grade and exhibits properties that support its performance under varying temperature conditions. According to ASTM D445, the kinematic viscosity of the oil is 109 cSt at 40°C and 14.7 cSt at 100°C, indicating its ability to maintain optimal flow characteristics over a broad temperature range. The viscosity index, measured using ASTM D2270, is 139, reflecting the oil's relatively stable viscosity with temperature changes. Furthermore, the oil demonstrates excellent thermal stability, with a pour point of -45°C and a flash point of 246°C, as determined by ASTM D92. These properties collectively make 15W40 oil a reliable choice for ensuring engine protection and performance in both cold and high-temperature operating environments.

Table 2 Specification of Base Oil

Parameter	Value
SAE Grade	15W40
Viscosity (ASTM D445)	
cSt @ 40º C	109
cSt @ 100 º C	14.7
Viscosity Index (ASTM D 2270)	139
Pour Point º C (ASTM D92)	-45
Flash Point º C (ASTM D92)	246

Nanoparticle Additives

To enhance the tribological properties of the base oil, Titanium Oxide (TiO_2) nanoparticles and Boron Nitride (BN) nanoparticles were selected as lubricant additives.

Titanium Oxide Dispersion (TiO_2)

Titanium Oxide Dispersion was procured from Gandhi Chemicals, Pune. It is a white powder with a particle size range of 10-20 nm and a purity of 99.9%. The dispersion uses propanol as a solvent and has a concentration of 15 wt% with a pH between 6 and 7. It exhibits a boiling point below 120°C, making it a suitable candidate for high-performance lubrication applications.

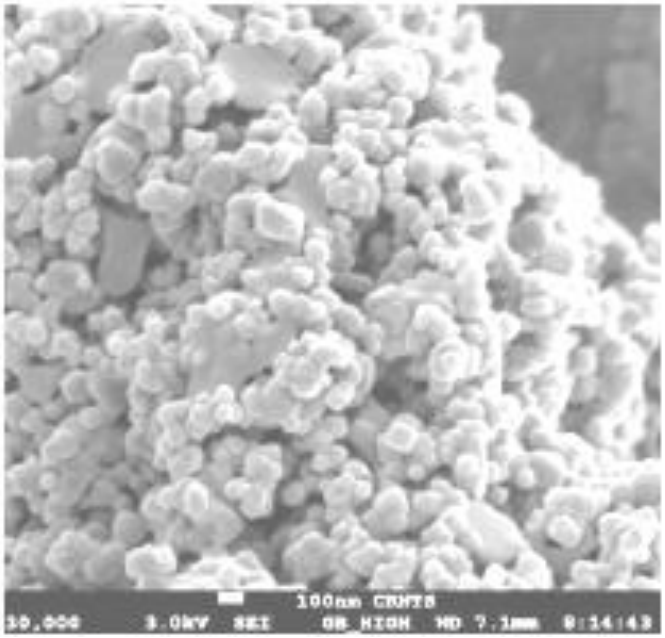

Fig. 1 Titanium Oxide Nanoparticles.

Boron Nitride Nanoparticles (BN)

Boron Nitride nanoparticles were sourced from Parshwaswami Metals, Mumbai. The selected BN nanoparticles are hexagonal in structure with an average particle size (APS) of 80 nm and a purity of 99.8%. The nanoparticles are white in color, possess a density of 2.29 g/cm³, and have an index of refraction of 1.74. They exhibit a thermal conductivity ranging from 40-120 W/mK, making them effective in heat dissipation applications. Additionally, BN nanoparticles have a coefficient of friction below 0.3 and a dielectric constant of 3-4, further improving their suitability as a lubricant additive.

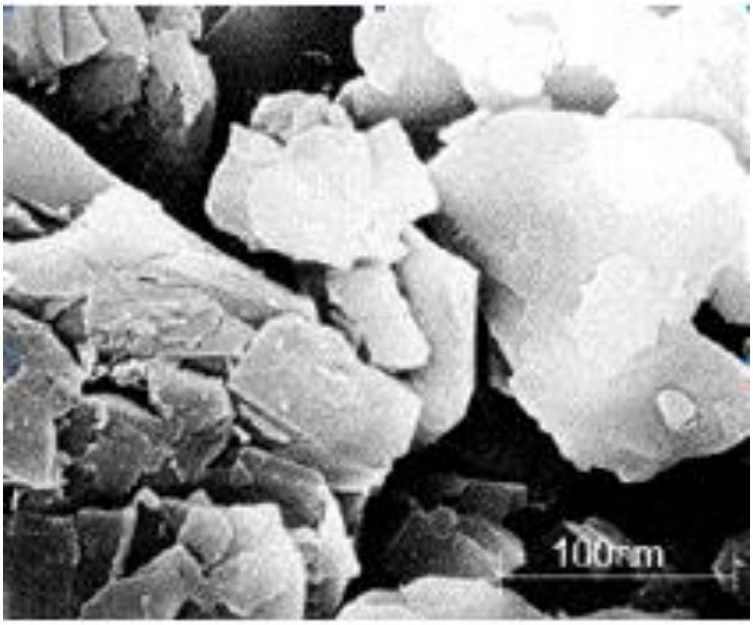

Fig. 2: SEM of Boron Nitride Nanoparticles.

Both nanoparticles were selected based on their excellent anti-wear, friction-reducing, and heat-resistant properties, which can enhance the overall performance of the 15W40 engine oil.

Sample Preparation

To evaluate the effect of TiO_2 and BN nanoparticles on the tribological properties of SAE 15W40 oil, different samples were prepared by varying the concentration of additives. The compositions of the formulated samples are listed in Table 2.

Table 3: Lubricant Sample Composition

Base Oil	Additives	% of Additives in Base Oil by Weight (g)	Sample No.
SAE 15W40	-	-	A
SAE 15W40	TiO_2 + hBN	0.1 + 0.05	B
SAE 15W40	TiO_2 + hBN	0.2 + 0.05	C
SAE 15W40	TiO_2 + hBN	0.3 + 0.05	D
SAE 15W40	TiO_2 + hBN	0.4 + 0.05	E
SAE 15W40	TiO_2 + hBN	0.3 + 0.02	F
SAE 15W40	TiO_2 + hBN	0.3 + 0.04	G
SAE 15W40	TiO_2 + hBN	0.3 + 0.06	H

The dispersion of nanoparticles in the base oil was carried out using mechanical stirring and agitation to ensure uniform suspension and to break down particle agglomerates. Propanol-2 was used as a surfactant during the dispersion process to prevent nanoparticle clustering and improve the stability of the formulation. This ensured an even distribution of nanoparticles within the oil, enhancing the tribological performance of the lubricant samples.

Fig. 4 Sample preparation.

Viscosity Analysis

The viscosity of the lubricant samples was measured at 40°C to evaluate the effect of TiO_2 and hBN nanoparticle additives on the base oil. The results are summarized in Table 19.

Table 4: Viscosity Summary at 40°C

Sample	TiO_2 (wt%)	hBN (wt%)	Viscosity (cSt) at 40°C
A (Base Oil)	0.00	0.00	106.78
B	0.10	0.05	107.89
C	0.20	0.05	108.77
D	0.30	0.05	110.44
E	0.40	0.05	112.01
F	0.30	0.02	109.89
G	0.30	0.04	110.11
H	0.30	0.06	110.89

The addition of TiO_2 and hBN nanoparticles resulted in a noticeable increase in viscosity across all samples. The viscosity of Sample D (TiO_2: 0.3 wt. %, hBN: 0.05 wt. %) increased by 3.66 cSt compared to the base oil (Sample A), indicating that nanoparticle additives enhance the oil's viscosity, potentially improving its load-bearing capacity and lubrication performance. The viscosity increase is influenced by both nanoparticle concentration and dispersion stability. Sample E (0.4 wt. % TiO_2) exhibited the highest viscosity (112.01 cSt), suggesting that higher nanoparticle concentrations further increase viscosity. However, excessive viscosity increments may impact oil flow and efficiency, requiring optimization based on application requirements.

EXPERIMENTAL

The tribological performance of the formulated lubricants was evaluated using a Four-Ball Extreme-Pressure (EP) Tester in accordance with ASTM D2783, Fig. 5. This test method determines the load-carrying capacity of lubricants by measuring the weld load, load-wear index, and scar diameters under extreme pressure conditions. The Four-Ball EP Tester consists of four chromium alloy steel balls with a uniform diameter of 12.7 mm. During testing, three steel balls are fixed within a test cup, while a fourth ball is held in a rotating chuck operating at 1770 rpm. The test lubricant and

equipment are maintained at a temperature range of 18°C to 35°C (65°F to 95°F).

Fig. 5 Four Ball Tester.

A series of tests are conducted with progressively increasing loads (6, 8, 10, 13, 16, 20, 24, 32, 40, 50, 63, 80, 100, 126, 160, 200, 250, 315, 400, 500, 620, and 800 kgf) until welding occurs—the point at which the balls fuse together due to excessive friction and heat.

Experimental Terminology

1. Hertz scar diameter: the average diameter in mm of an indentation caused by the deformation of balls under static load (prior to test) is

$$DH = 8.73 \times p^{1/3}$$

Where, DH = hertz diameter of the contact area

p = static applied load.

Fig. 6 Example of Scar Diameter.

2. Corrected load: calculation and record for each applied load between the last no seizure. Load and weld point using the equation.

$$\text{Corrected load (kg-f)} = {}^{L \times Dh}/_{X}$$

Where, l = applied load (kgf).

dh = hertz scar diameter (mm)

x = average scar diameter (mm)

3. Load-Wear index: calculate and record the load-wear index in kg-f

Using the equation:

Load-wear index (kg-f) = $\frac{A}{10}$

Where, a sum of the corrected loads determined for the ten applied loads immediately preceding the weld point.

RESULTS & DISCUSSION

Wear Test

Wear test carried out as per prepared samples. Observation for the experiments are as below

Ball 1

Ball 2

Ball 3

Fig. 7 Ball Scar Images for Ball 1, Ball 2 and Ball 3 of Tribotester using sample A

Figure 7 presents the optical images of wear scars on Ball 1, Ball 2, and Ball 3 obtained from tribological testing of Sample A. The images reveal the extent of surface degradation and wear patterns developed during the test. Each ball shows a clear elliptical wear scar outlined in red, indicating the contact region subjected to sliding and friction. The similarity in scar shape and orientation suggests consistent loading and relative motion during testing. However, slight variations in scar size and surface texture can be observed, which may point to localized differences in material response or lubrication conditions. These wear scars serve as critical indicators for evaluating the performance of lubricants and the tribological behavior of the material pair under test.

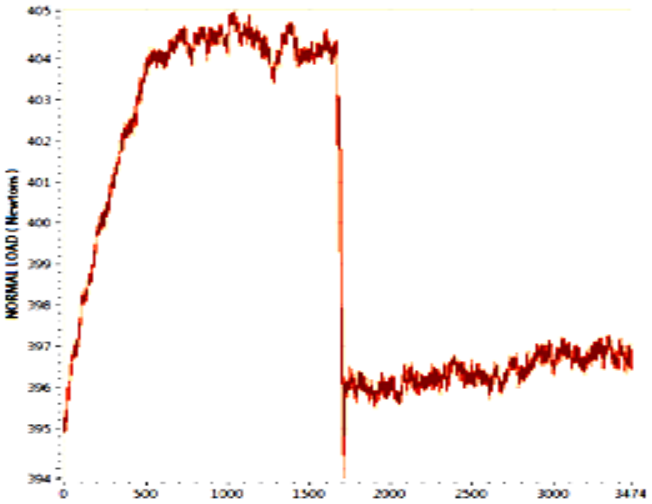

Fig. 8: Normal Load (Newtons) Vs Time for Sample A.

Figure 8 illustrates the variation of normal load (in Newtons) with respect to time during the tribological testing of Sample A. The graph exhibits an initial increase in normal load, reaching a peak of approximately 404 N around the 1000-second mark. This rise indicates the load ramp-up phase, where the system stabilizes to the intended testing conditions. Following the peak, a sudden drop is observed, likely due to a system adjustment or transient event, after which the load stabilizes around 396–398 N for the remainder of the test duration. The relatively stable load profile post-transient suggests consistent test conditions and reliable contact between the tribo-pairs, essential for accurate evaluation of wear and frictional behavior. This load-time profile confirms the integrity and control of the testing setup throughout the experiment.

Figure 9 shows the variation of frictional torque (in N·m) with time for Sample A during the tribological test. The graph exhibits a steady rise in frictional torque from the start, peaking at approximately 0.18 N·m around 1200 seconds. This initial increase corresponds to the system reaching stable sliding conditions under load. After reaching its peak, the torque gradually decreases and stabilizes between 0.15 and 0.16 N·m for the remainder of the test duration. This trend suggests the onset of a steady-state wear regime, where the contact surfaces have undergone sufficient conformal wear and the lubrication effect, if present, has reached equilibrium. Minor fluctuations throughout the test reflect dynamic surface interactions such as asperity deformation or lubricant film variation. Overall, the frictional torque profile supports the presence of stable tribological behavior in Sample A under sustained testing conditions.

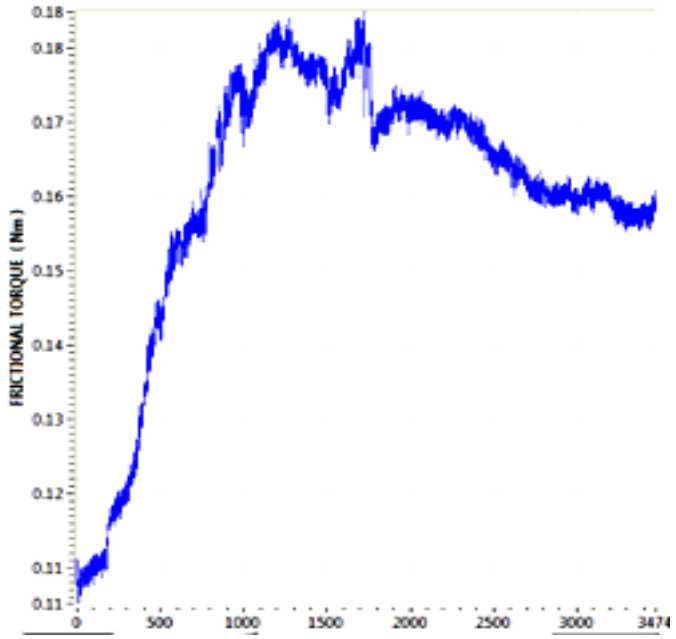

Fig. 9 Frictional Torque (Nm) Vs Time for Sample A.

Summary of Wear Test

Table 5 - Wear test Summary

Sample Details			Viscosity (cSt) at 40°C	Mean Diam			Average scar dia, µm	Scar Area			Average scar area, mm²
		%		Ball 1	Ball 2	Ball 3		Ball 1	Ball 2	Ball 3	
A	TiO2	0	106.78	462	514	470	482.0	0.167	0.206	0.172	0.182
	hBN	0									
B	TiO2	0.1	107.89	359	354	386	366.3	0.1	0.097	0.116	0.104
	hBN	0.05									
C	TiO2	0.2	108.77	462	480	498	480.0	0.166	0.178	0.194	0.179
	hBN	0.05									
D	TiO2	0.3	110.44	382	348	357	362.3	0.114	0.095	0.1	0.103
	hBN	0.05									
E	TiO2	0.4	112.01	455	428	454	445.7	0.162	0.142	0.11	0.155
	hBN	0.05									
F	TiO2	0.3	109.89	462	442	473	459.0	0.167	0.152	0.174	0.164
	hBN	0.02									
G	TiO2	0.3	110.11	346	332	339	339.0	0.093	0.086	0.09	0.090
	hBN	0.04									
H	TiO2	0.3	110.89	352	371	363	362.0	0.09	0.107	0.103	0.102
	hBN	0.06									

The four-ball tribotester results demonstrate the influence of TiO_2 and hBN additives on the tribological performance of the tested samples, Fig. 10. The reference sample (A) exhibited the highest wear, with an average scar diameter of 482.0 µm and a scar area of 0.182 mm², indicating poor wear resistance. In contrast, the addition of TiO_2 and hBN significantly reduced wear, with the best performance observed in Sample G (TiO_2 0.3%, hBN 0.04%), which exhibited the lowest scar diameter (339.0 µm) and scar area (0.090 mm²). Other optimized compositions, such as Samples B, D, and H, also demonstrated improved wear resistance.

Figure 11 illustrates the variation in mean scar area (mm²) as a function of TiO_2 concentration (%) for samples B, C, D, and E, with a fixed hexagonal boron nitride (hBN) content of 0.05%. The trend reveals a non-linear relationship between TiO_2 concentration and wear performance. At 0.1% TiO_2, the mean scar area is approximately 0.10 mm², which increases to a peak value of around 0.17 mm² at 0.2% TiO_2, indicating a rise in wear. Interestingly, a further increase in TiO_2 to 0.3% results in a significant reduction in scar area to nearly 0.10 mm², suggesting improved anti-wear behavior at this composition. However, at 0.4% TiO_2, the scar area increases again to about 0.15 mm². These findings suggest that the optimal TiO_2 concentration for minimizing wear lies around 0.3%, and both lower and higher concentrations may compromise the tribological performance, possibly due to particle agglomeration or suboptimal dispersion within the lubricant matrix.

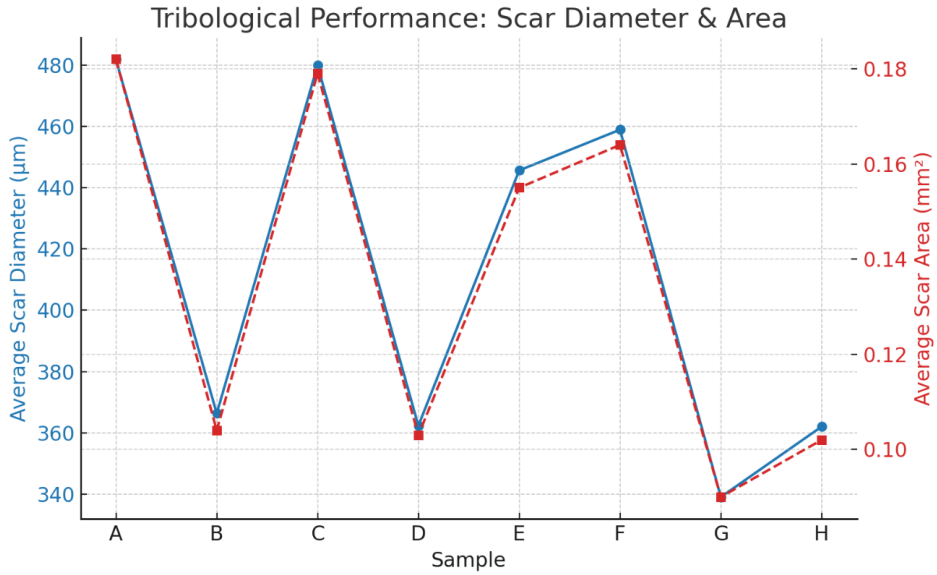

Fig. 10 Average scar diameter for various samples.

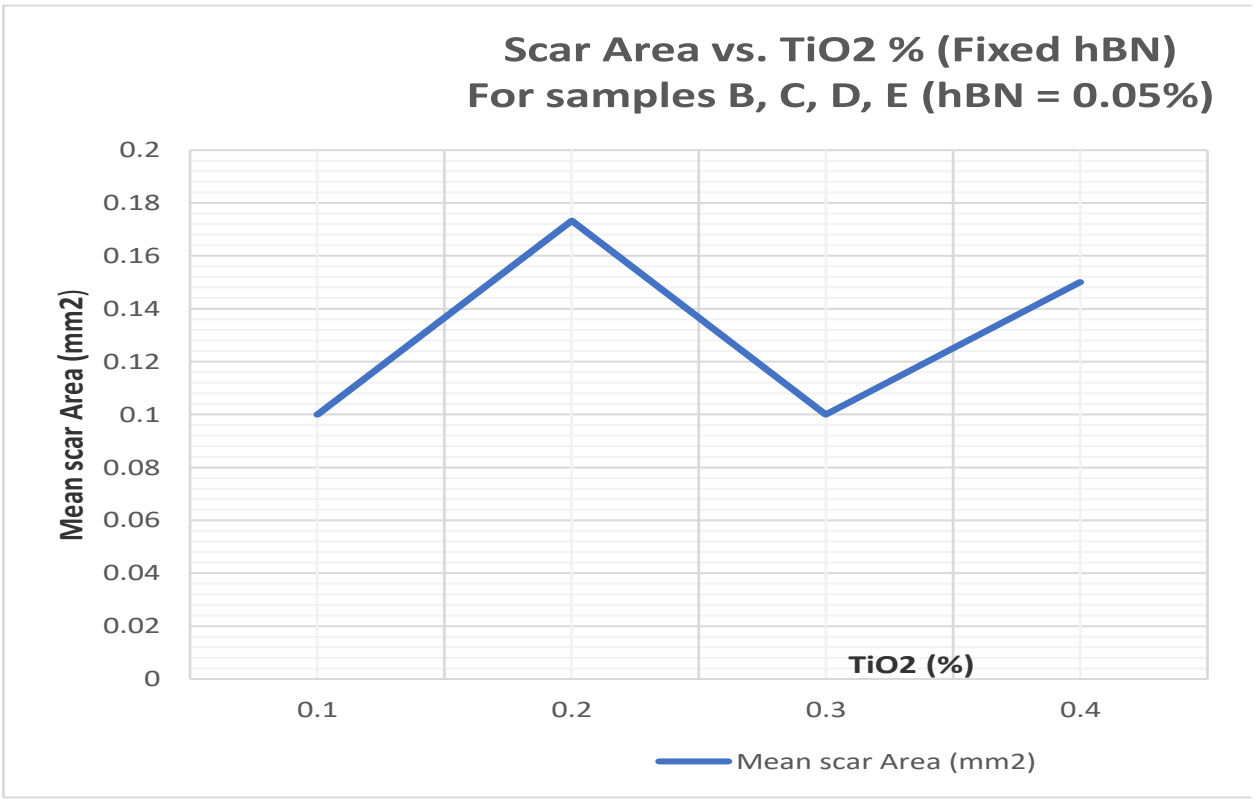

Fig. 11 Mean scar area for various TiO2 % with fixed hBN %.

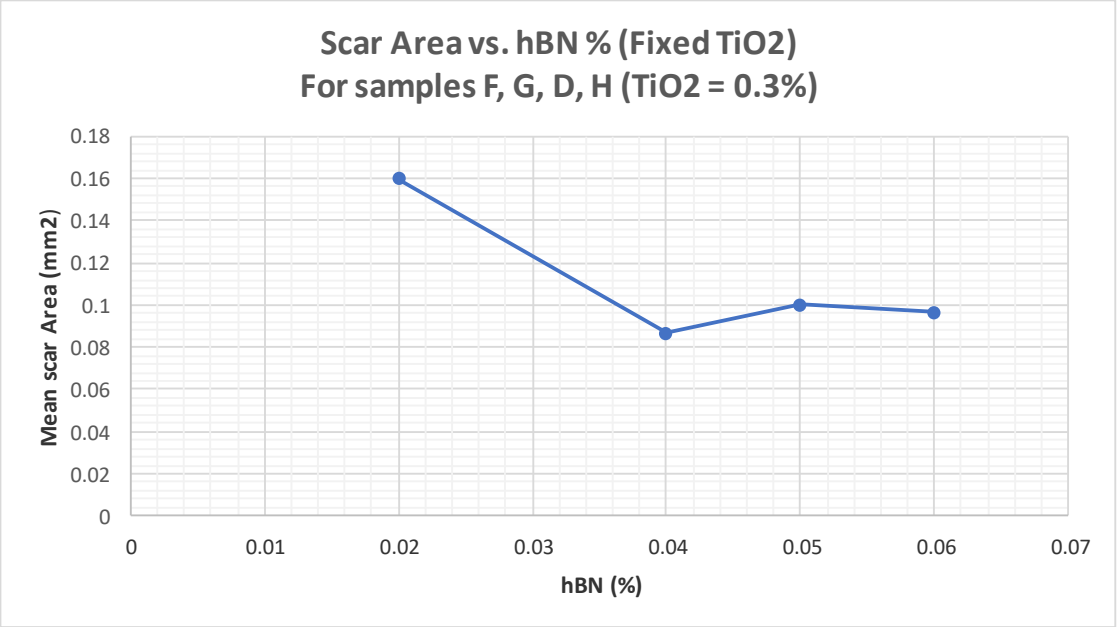

Fig. 12 Mean scar area for various hBN % with fixed TiO_2 %.

Figure 12 illustrates the effect of varying hexagonal boron nitride (hBN) content on the mean scar area (mm^2) for samples F, G, D, and H, while maintaining a constant TiO_2 concentration of 0.3%. The data reveal a clear trend in which increasing hBN

content initially leads to a significant reduction in wear scar area. At 0.01% hBN, the scar area is highest, approximately 0.16 mm². As the hBN concentration increases to 0.04%, the scar area decreases sharply to around 0.08 mm², indicating enhanced anti-wear performance likely due to the lubricating and load-bearing properties of hBN. Beyond this concentration, however, a slight increase in scar area is observed, with values stabilizing around 0.09–0.10 mm² for 0.05% and 0.06% hBN. This suggests that while moderate additions of hBN improve tribological behavior, excessive amounts may lead to particle agglomeration or reduced dispersion efficiency, thereby limiting further improvements. Overall, 0.04% hBN appears to be the optimal concentration for minimizing wear under the given conditions.

Comparison of Wear Test Results
Comparison between Experiment A-D-G

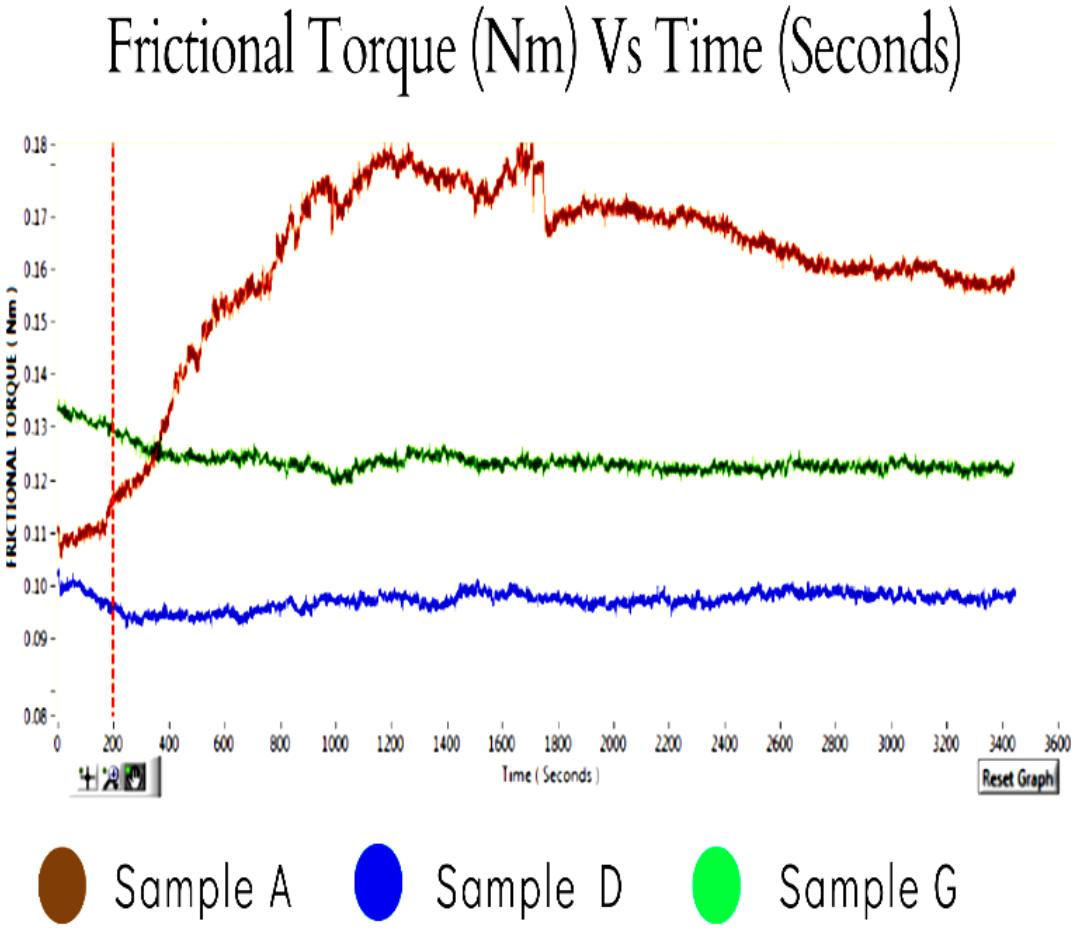

Fig. 13 Comparison of experiments A-D-G.

Figure 13 presents a comparative analysis of frictional torque (Nm) over time (seconds) for Samples A, D, and G. The graph clearly shows distinct performance trends among the samples, reflecting the influence of additive composition on tribological behavior. Sample A (brown), the base sample without additives, exhibits the highest frictional torque throughout the test, peaking at approximately 0.177 Nm. This indicates significant resistance to sliding, consistent with higher wear and

energy dissipation.

In contrast, Sample D (blue), which contains a combination of 0.3% TiO_2 and 0.05% hBN, shows the lowest and most stable frictional torque, around 0.095 Nm, highlighting the synergistic lubricating and load-bearing effects of the hybrid nanoparticle formulation. Sample G (green), containing 0.3% TiO_2 and 0.01% hBN, displays intermediate frictional torque values (~0.125 Nm), higher than Sample D but significantly lower than Sample A. These results suggest that increasing the hBN concentration to an optimal level improves tribological performance by minimizing friction and wear. Overall, the data underscore the effectiveness of nanoparticle additives—particularly in balanced combinations—in reducing frictional losses under sliding conditions.

4.3.2 Comparison between Experiment B-C-D-E

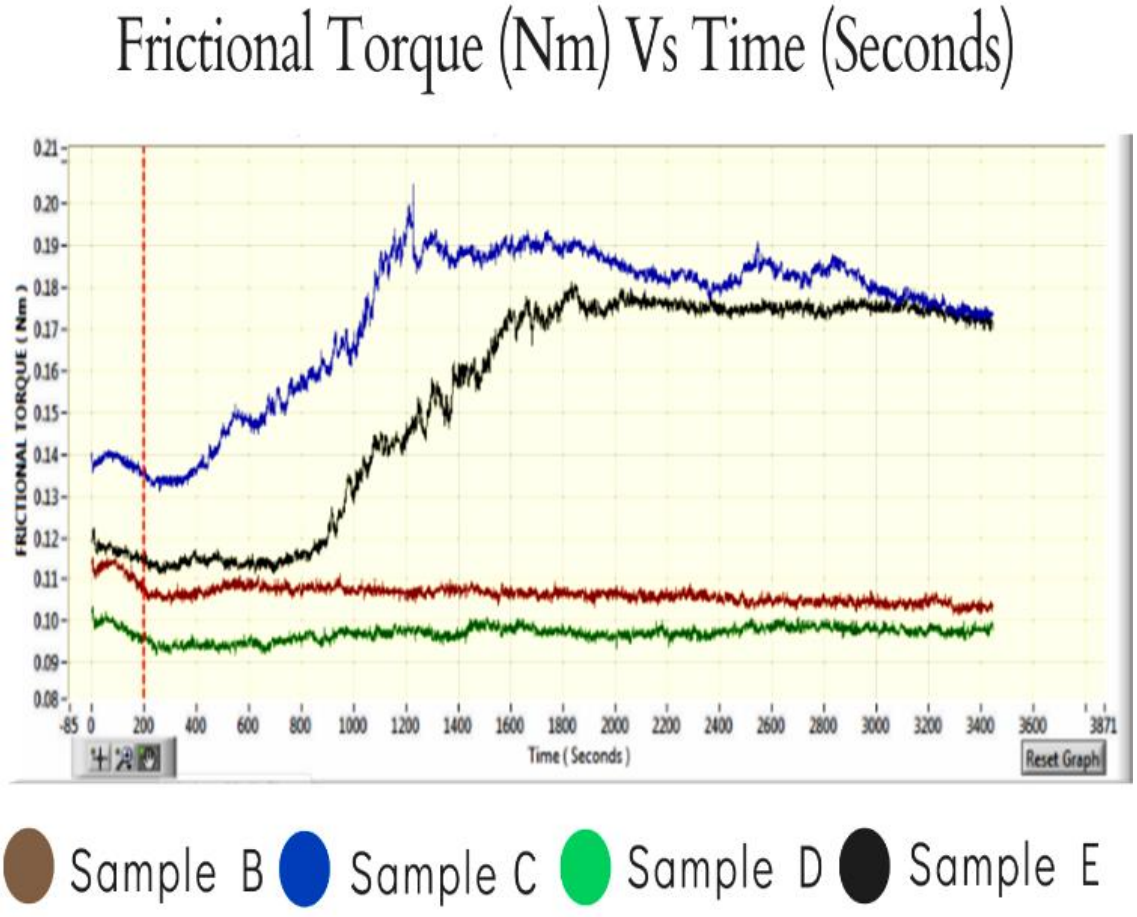

Fig. 14 Comparison of experiments B-C-D-E.

Figure 14 illustrates the variation of frictional torque with time for Samples B, C, D, and E, highlighting the influence of TiO_2 concentration on tribological performance at a fixed hBN content (0.05%). Among the tested samples, Sample C (blue), containing 0.2% TiO_2, exhibited the highest frictional torque values, peaking near 0.195 Nm. This suggests increased resistance to motion and potentially higher wear under these conditions. Sample E (black), with the highest TiO_2 concentration

(0.4%), also showed elevated frictional torque (~0.175 Nm), though slightly lower than Sample C. In contrast, Sample D (green), containing 0.3% TiO_2, consistently demonstrated the lowest frictional torque (~0.095 Nm), indicating optimal performance in reducing friction. Sample B (brown), with 0.1% TiO_2, displayed intermediate torque behavior (~0.11 Nm), showing moderate improvement compared to the unoptimized sample C.

The data suggests that a TiO_2 concentration of 0.3% in the presence of 0.05% hBN offers the most favorable balance between anti-frictional and wear-resisting characteristics. Excessive or insufficient TiO_2 concentrations appear to hinder performance, possibly due to nanoparticle agglomeration or inadequate surface coverage. These findings reinforce the importance of compositional optimization for effective tribological enhancement using hybrid nanoparticle additives.

Comparison of Experiments F-G-H

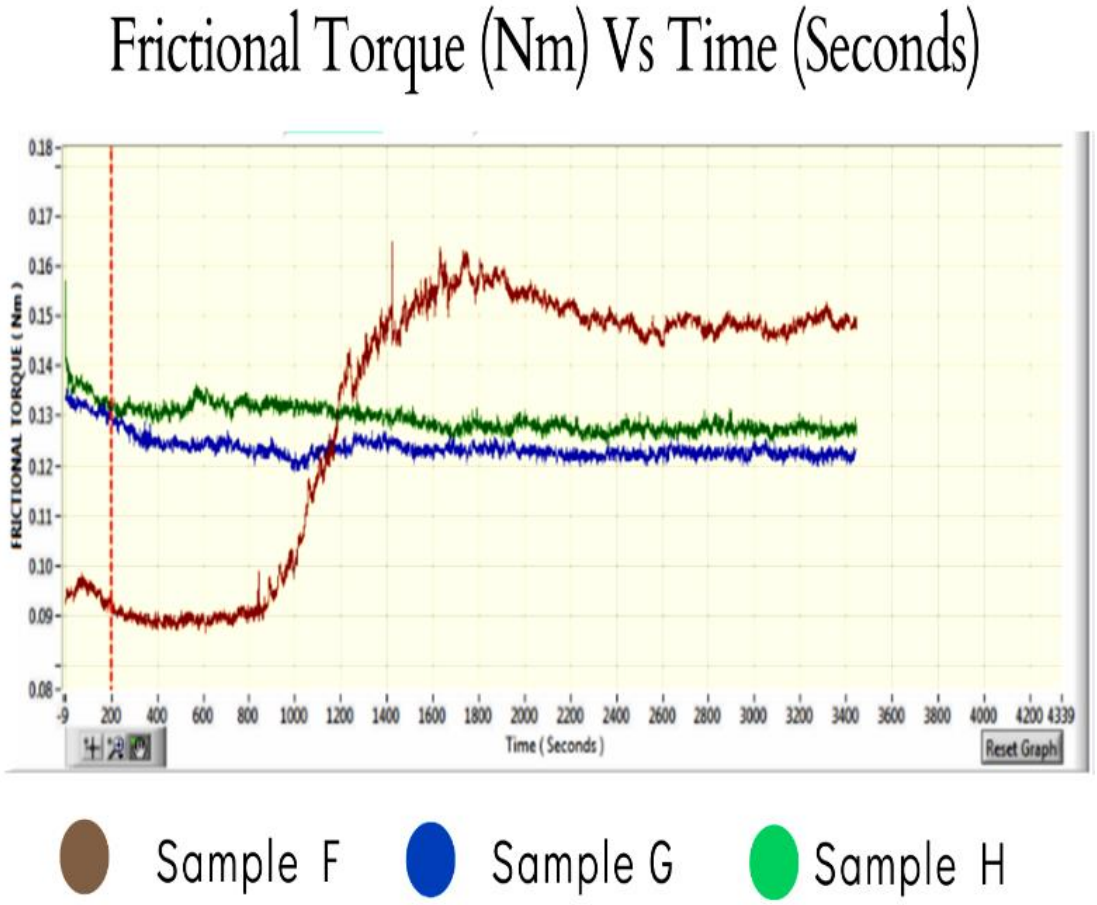

Fig. 15 Comparison of experiments F-G-H.

Figure 15 presents the frictional torque behavior over time for Samples F, G, and H, providing insight into the tribological response at a fixed TiO_2 concentration (0.2%) with varying hBN content. Sample F (brown), containing no hBN, exhibits the highest frictional torque values, rising sharply after ~1100 seconds and stabilizing around 0.155 Nm. This elevated torque suggests increased surface resistance and possible wear propagation due to the absence of solid lubricant.

In contrast, the introduction of hBN markedly improves tribological performance. Sample G (blue), with 0.05% hBN, demonstrates a significant reduction in frictional torque, maintaining values around 0.12 Nm throughout the test duration. Further enhancement is observed in Sample H (green), which contains 0.1% hBN, showing the lowest and most stable torque (~0.13 Nm initially, reducing slightly over time), indicating improved lubrication and reduced interfacial shear stress.

The comparative performance underscores the synergistic role of hBN in reducing friction when combined with TiO_2. While Sample F experienced substantial frictional buildup, the presence of hBN in Samples G and H effectively suppressed torque rise, confirming the additive's role in enhancing film-forming capability and load-carrying capacity under tribological stress.

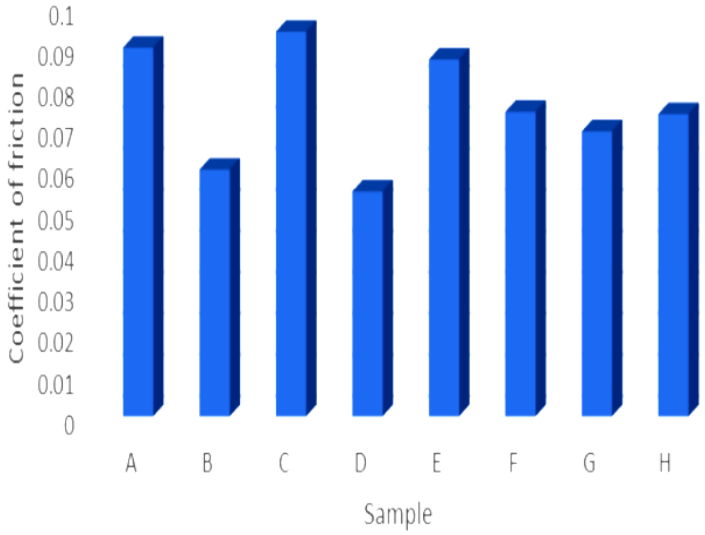

Fig. 16 Coefficient of friction for various samples.

The frictional torque vs time analysis across all tested samples (A to H) reveals the critical influence of additive composition—specifically TiO_2 and hBN nanoparticles—on the tribological performance of the lubricant system. Samples without hBN (such as A, B, and F) consistently exhibited higher and more unstable frictional torque over time, suggesting increased surface resistance and a lack of effective lubrication. This behavior points to accelerated wear or thermal degradation under sustained operation. In contrast, samples containing hBN (particularly C, E, G, and H) showed significant improvement in frictional stability and lower overall torque values. Notably, Sample C (0.1% hBN + 0.2% TiO_2) demonstrated the lowest and most stable frictional response (~0.18–0.19 Nm), indicating excellent load-bearing capacity and film-forming behavior. Sample E also exhibited superior performance, confirming the beneficial synergistic effect of hBN in enhancing boundary lubrication and reducing frictional losses.

Among the samples with lower hBN content (G and H), there was a marked improvement over their non-hBN counterparts, reinforcing that even a small fraction of hBN contributes positively to reducing torque and maintaining stability over extended test durations. Overall, the results clearly demonstrate that the combined use of TiO_2 and hBN additives significantly enhances the tribological

behavior of lubricants. Higher concentrations of hBN, in particular, lead to reduced friction, improved stability, and prolonged system integrity, making these formulations highly promising for applications requiring efficient and durable lubrication under dynamic loading conditions.

ANOVA Analysis of Mean Scar Area Across Different Samples

An analysis of variance (ANOVA) was conducted to statistically evaluate the differences in mean scar areas among the tested lubricant samples (A–H), each with three replicates. The primary objective was to determine whether the variations in scar area were significantly influenced by the composition of the lubricant additives, specifically TiO_2 and hBN. The overall mean scar area was calculated to be approximately 0.1304 mm^2.

Table 6 ANOVA Analysis of Mean Scar Area Across Different Samples

Sample	Mean Scar Area (mm2)	Between-Group Sum of Squares (SSB) (mm) SSB = Σ [n * (group mean - overall mean)²], where n = 3 (replicates per sample)	Within-Group Sum of Squares (SSW) (mm) SSW = Σ (observation - group mean)² for all observations
A	0.1767	0.006426	0.000866
B	0.1	0.002772	0.0002
C	0.1733	0.005523	0.000466
D	0.1	0.002772	0.0002
E	0.15	0.001152	0.0002
F	0.16	0.002628	0.0002
G	0.0867	0.005727	0.000067
H	0.0967	0.003408	0.000067
Total	- Overall mean = 3.13 / 24 ≈ 0.1304 mm	SSB = 0.006426 + 0.002772 + 0.005523 + 0.002772 + 0.001152 + 0.002628 + 0.005727 + 0.003408 ≈ 0.030408	SSW = 0.000866 + 0.0002 + 0.000466 + 0.0002 + 0.0002 + 0.0002 + 0.000067 + 0.000067 ≈ 0.002266

The between-group sum of squares (SSB) was found to be approximately 0.030408, indicating considerable variation among the group means. In contrast, the within-group sum of squares (SSW) was significantly lower at 0.002266, reflecting relatively low variation within each sample group. This large disparity between SSB and SSW strongly suggests that the observed differences in scar area are primarily

due to the differences in sample formulation rather than random experimental error.

Notably, samples G and H both containing hBN recorded the lowest mean scar areas (0.0867 mm² and 0.0967 mm² respectively), highlighting the effective anti-wear properties of hBN. On the other hand, Sample A exhibited the highest mean scar area (0.1767 mm²), indicating higher wear when hBN was absent. These findings are consistent with the frictional torque analysis, further validating the tribological benefits of incorporating hBN nanoparticles into lubricant formulations.

Table 7 Anova Analysis Result Table

Source	Sum of Squares	Degree of Freedom df	Mean Square	F Statistics	P Value
Between Groups	0.0304	7	0.0043	30.62	< 0.001
Within Groups	0.0023	16	0.0001		
Total	0.0327	23			

The significant F-statistic (30.62, $p < 0.001$) confirms that the additive compositions (TiO_2 and hBN percentages) influence wear performance, as measured by scar area. When TiO_2 is fixed at 0.3%, increasing hBN from 0.02% to 0.04% reduces scar area (from 0.1600 mm^2 to 0.0867 mm^2), but further increases to 0.06% slightly raise it (0.0967 mm^2), hinting at an optimal hBN level around 0.04%. TiO_2's effect is less consistent, with no monotonic trend. Overall, the ANOVA results provide strong statistical evidence supporting the hypothesis that the inclusion of hBN, either alone or in synergy with TiO_2, leads to a significant reduction in wear, as reflected by the reduced scar areas.

CONCLUSIONS

In the present research, properties of lubricating oil 15W40 is evaluated by addition of TiO_2 and hBN nano particle with various blending combinations of concentrations.

The following conclusions are obtained from experimental results.

1 The tribological test shows that sample D (0.3% of TiO_2 + 0.05% of hBN additives in 15W40 oil) is the best sample among all the prepared samples when compared with Sample A (base oil without additives).

2 The tribological test shows that sample D (0.3% of TiO_2 + 0.05% of hBN additives in 15W40 oil) shows 43% improvement in wear properties with respect to Sample A (base oil without additives)

3 The tribological test for load carrying capacity shows that sample D (0.3% of TiO_2 + 0.05% of hBN additives in 15W40 oil) shows 25% improvement in load

carrying capacity with respect to Sample A (base oil without additives). Weld load for sample D is 200Kg where weld load for base oil is 160 Kg.

4 The tribological test for coefficient of frictionshows that sample D (0.3% of TiO_2 + 0.05% of hand additives in 15W40 oil) shows 39% improvement in coefficient of friction with respect to Sample A (base oil without additives)

5 It is observed that viscosity of Sample D is increased by 3.4% over Sample A(base oil without additives).

6 Furthurmore, ANOVA results provide strong statistical evidence supporting the hypothesis that the inclusion of hBN, either alone or in synergy with TiO_2, leads to a significant reduction in wear, as reflected by the reduced scar area.

REFERENCES

1. Bhaumik, Shubrajit & Pathak, S.D.. (2016). A Comparative Experimental Analysis of Tribological Properties Between Commercial Mineral Oil and Neat Castor Oil using Taguchi Method in Boundary Lubrication Regime. Tribology in Industry. 38. 33-44.

2. D. Md Razak, S. Syahrullail, Azli Yahya, Nazriah Mahmud, Nor Liyana Safura Hashim, Kartiko Nugroho, Lubrication on the Curve Surface Structure Using Palm Oil and Mineral Oil, Procedia Engineering, Volume 68, 2013, Pages 607-612, ISSN 1877-7058, https://doi.org/10.1016/j.proeng.2013.12.228.

3. D, Mahipal & P., Krishnanunni & P, Mohammed & N H, Jayadas. (2014). Analysis of lubrication properties of zinc-dialkyl-dithio-phosphate (ZDDP) additive on Karanja oil (Pongamia pinnatta) as a green lubricant. International Journal of Engineering Research. 3. 494-496. 10.17950/ijer/v3s8/804.

4. Laad, Dr & Jatti, Vijaykumar. (2016). Titanium oxide Nanoparticles as Additives in Engine oil. Journal of King Saud University - Engineering Sciences. 30. 10.1016/j.jksues.2016.01.008.

5. Ilie, F., & Covaliu, C. (2016). Tribological Properties of the Lubricant Containing Titanium Dioxide Nanoparticles as an Additive. Lubricants, 4(2), 12. https://doi.org/10.3390/lubricants4020012

6. Dighe Yogesh S, Pandharkar Ujjawala J, Investigate the load carrying capacity of SAE 40 lubricating oils without using extreme pressure additives on four ball extreme pressure oil testing machine, International Advanced Research Journal in Science, Engineering and Technology, Vol. 3, Special Issue 1, March 2016.

7. S. Syahrullail, S. Kamitani, A.Shakirin, Performance of Vegetable Oil as Lubricant in Extreme Pressure Condition, Procedia Engineering 68 (2013) 172 – 177.

8. David W. Johnson and John E. Hils, Phosphate Esters, Thiophosphate Esters and Metal Thiophosphates as Lubricant Additives, Lubricants2013, 1, 132-148.

9. He, J. Q., Zhang, L., & Wang, X. (2023). Synergistic tribological enhancement of N-doped carbon quantum dots and MoS_2 nanofluid additives in lubricants. *Wear*, *522*, 204876. https://doi.org/10.1016/j.wear.2023.204876

10. V.S. Mello, E.A. Faria, S.M. Alves, C. Scandian, Enhancing Cuo nanolubricant performance using dispersing agents, Tribology International, Volume 150, 2020, 106338, ISSN 0301-679X, https://doi.org/10.1016/j.triboint.2020.106338.

11. Patel, J., Kumar, N., & Shah, S. R. (2023). Graphene-enhanced palm oil-based nanofluids for automotive lubrication. *Journal of Cleaner Production*, *415*,

137789. https://doi.org/10.1016/j.jclepro.2023.137789
12. Wan, Zhongyu & Wang, Quande & Liu, Dongchang & Liang, Jinhu. (2021). Discovery of ester lubricants with low coefficient of friction on material surface via machine learning. Chemical Physics Letters. 773. 138589. 10.1016/j.cplett. 2021.138589.
13. Zhang, Kaipeng & Tang, Hongtao & Shi, Xiaoliang & Xue, Yawen & Huang, Qipeng. (2023). Effect of Ti3C2 MXenes additive on the tribological properties of lithium grease at different temperatures. Wear. 526-527. 204953. 10.1016/j.wear. 2023.204953.